Available online at www.sciencedirect.com
SCIENCE DIRECT®
ELSEVIER
Nuclear Instruments and Methods in Physics Research B 243 (2006) 200–204
NIM B Beam Interactions with Materials & Atoms
www.elsevier.com/locate/nimb

Ion beam analysis of PECVD silicon oxide thin films

F. Fernandez-Lima [a], J.A. Rodriguez [b], E. Pedrero [b], H.D. Fonseca Filho [c], A. Llovera [d], M. Riera [d], C. Dominguez [d], M. Behar [e,*], F.C. Zawislak [e]

[a] Instituto Superior de Tecnologías y Ciencias Aplicadas, Ave Salvador Allende esq Luaces, s/n, C.P. 10600, Ciudad de la Habana, Cuba
[b] Facultad de Física – IMRE, Universidad de la Habana, Cuba
[c] Departamento de Física, Pontifícia Universidade Católica do, Rio de Janeiro, Brazil
[d] Instituto de Microelectrónica de Barcelona, España, Spain
[e] Instituto de Física, Universidade Federal do Rio Grande do Sul, Av. Bento Goncalves 9500, C.P. 15051, 91501-970 Porto Alegre, Brazil

Received 13 June 2005; received in revised form 26 July 2005
Available online 28 November 2005

Abstract

A study of ion beam analysis techniques of plasma enhanced chemical vapor deposited (PECVD) silicon oxide thin films (1 μm thick) obtained from silane (SiH_4) and nitrous oxide (N_2O) is reported. The film, elemental composition and surface morphology were determined as function of the reactant gas flow ratio, $R = [N_2O]/[SiH_4]$ in the 22–110 range using the Rutherford backscattering spectrometry, nuclear reaction analysis and atomic force microscopy techniques. The density of the films was determined by combining the RBS and thickness measurements. All the experiments were done at a deposition temperature of 300 °C. In all the cases almost stoichiometric oxides were obtained being the impurity content function of R. It was also observed that physical properties such as density, surface roughness and shape factor increase with R in the studied interval.
© 2005 Elsevier B.V. All rights reserved.

PACS: 82.80.Yc; 68.37.Ps; 81.05.Je

Keywords: Ion beam analysis; Silicon oxide; RBS; AFM

1. Introduction

The use of silicon oxide thin films obtained from silane (SiH_4) and nitrous oxide (N_2O) by plasma enhanced chemical vapor deposition (PECVD) technique has significantly grown in the last years. Improved physical properties, low deposition temperatures (<400 °C) and the presence of dangling bonds for the gettering of water molecules through the oxide [1] make these layers very attractive for silicon integrated circuit technology. Indeed, they are widely employed in very and ultra large scale integration microelectronic devices, as inter-metal dielectric (IMD) layers and in the construction of micro-electro mechanical systems (MEMS) components, positively impacting the microelectronic industry [1–3].

Due to the deposition reactions, impurities such as hydrogen, nitrogen, and water are introduced in the films during the deposition process. Moreover, moisture is generally incorporated from the atmosphere after deposition. As a result, in addition to the normal Si–O bonds, Si–H, Si–OH, Si–N, H–O–H and N–H bonds as well as other non-bonded species (i.e. trapped nitrogen or hydrogen molecules) are present in the films. The deterioration of the film quality is a function of the type and concentration of the present impurities which in turn is strongly dependent on the precursor gas flow ratio R, defined as $R = [N_2O]/[SiH_4]$. Therefore, the evaluation of the film composition as a function of R is of the utmost importance.

Most of the above mentioned impurities can be detected by techniques such as Fourier transform infrared

* Corresponding author. Tel.: +55 51 3316 7111; fax: +55 51 3316 7286.
E-mail address: behar@if.ufrgs.br (M. Behar).

0168-583X/$ - see front matter © 2005 Elsevier B.V. All rights reserved.
doi:10.1016/j.nimb.2005.07.244

spectroscopy (FTIR), X-ray photoelectron spectroscopy (XPS) and others. However non-bonded (trapped) hydrogen requires a different technique to be detected.

In a previous paper [4] we studied the effect of H-related impurities on the thermal behavior of the stress in PECVD silicon oxide films. Different impurity species were qualitatively evaluated by the analysis of FTIR spectra for a wide range of R-values.

In the present paper, a full quantitative study, using ion beam analysis (IBA) techniques, of PECVD silicon oxide thin films is reported. The film was obtained from silane and nitrous oxide, as a function of the reactant gas flow ratio, at a constant deposition temperature of 300 °C. The main emphasis is made for R-values in the 22–110 range since almost stoichiometric oxides were estimated to be produced in this interval [4]. The film, stoichiometry and concentration of Si, O, N and H as well as their depth distribution were determined by Rutherford backscattering spectrometry (RBS) and nuclear reaction analyses (NRA) techniques. The density of the films was determined combining the RBS technique with thickness measurements. The oxide film topography was analyzed using atomic force microscopy (AFM).

2. Sample preparation

The deposition processes were achieved on a large radial flow capacitively coupled parallel-plate PECVD reactor, operated at 13.56 MHz. Details of the installation can be found elsewhere [5]. Undiluted silane and nitrous oxide were used as precursors. Chamber pressure, r.f. power density and nitrous oxide flow during depositions were fixed at 0.2 Torr, 30 W/cm^2 and 110 sccm, respectively. The [N_2O]/[SiH_4] flow ratio was varied in the 22–110 interval and the substrate temperature was fixed at 300 °C. The films were deposited on one-side polished p-type (14–20 Ω cm) silicon (1 0 0) wafers.

3. Film characterization

3.1. Film composition and density

The quantitative analysis of the elements present in the films and their depth distribution was done by using ion beam analysis (IBA) techniques, selected according to its sensitivity to the elements to be measured, i.e. H, Si, O and N. The analyses have been performed using the 3 MV Tandetron accelerator of the Institute of Physics, Federal University of Rio Grande do Sul, Brazil.

The Rutherford backscattering spectrometry (RBS) was used to measure the Si and O content by means of a 2.0 MeV $^4He^+$ beam. A surface barrier detector located at 165° with respect to the incident beam was used to detect the backscattered ions. The overall resolution of the detector plus the associated electronics was better than 13 keV (FWHM). The RBS spectra were analyzed using the Rump program [6] (see Fig. 1). From the fit obtained with the

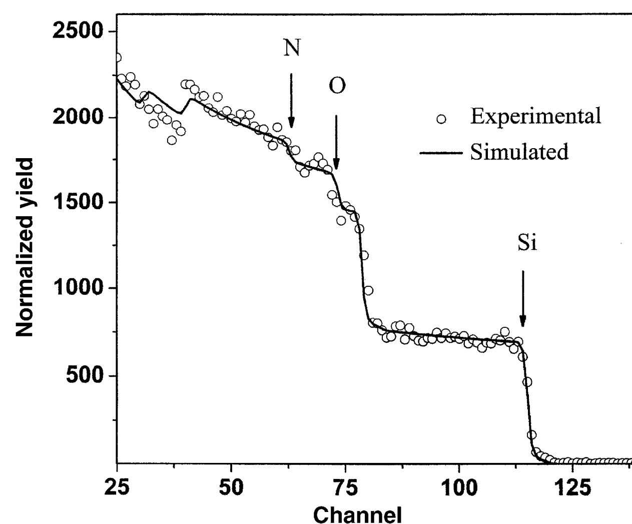

Fig. 1. 2.0 MeV $^4He^+$ RBS spectrum (dots) and the simulation (full line) for one of the analyzed samples.

Table 1
Density and composition in terms of percentage of each atomic species of the SiO_x(N:H) studied samples

R	Density (10^{22} atom/cc)	RBS stoichiometry			Atomic (%)			
		Si	O	N	Si	O	N	H
22	4.24	1	1.8	1.3	13	25	17	45
55	7.49	1	2	0.25	21	42	5	32
73.2	9.25	1	1.8	0.6	22	39	13	26
110	9.74	1	2	0.2	22	45	5	28

Typical errors are ±5%.

Rump algorithm we were able to determine for each R value the Si–O–N stoichiometries which are quoted in Table 1, column 3. The corresponding densities were obtained combining the RBS data with the thickness values of the film obtained by using a Rudolph Research Auto EI IV ellipsometer operating at 632.8 nm and 70° incidence angle. The density values as a function of R are quoted in column 2 of Table 1.

In addition we have used the $^{16}O(\alpha,\alpha)^{16}O$ elastic reaction at $E_r = 3035$ keV as a complementary way of determining the O concentration. Fig. 2 shows the yield of the O peak obtained at the resonance energy as a function of the ratio R. As can be observed with exception of the lower R value, the O yield remains almost constant. The transformation from the oxygen yield to concentration was performed using a well defined standard. The obtained results are completely consistent with those obtained from the fitting of the RBS spectra by the Rump program.

The hydrogen and nitrogen concentrations were determined using NRA techniques. The H concentration was measured through the $^{15}N(H;\alpha,\gamma)^{12}C$ nuclear resonant reaction at $E_r = 6385$ keV. The emitting gamma rays were detected by a 2 in. × 2 in. BGO cintillator situated at 4 cm from the target. The gamma yields for different R-values,

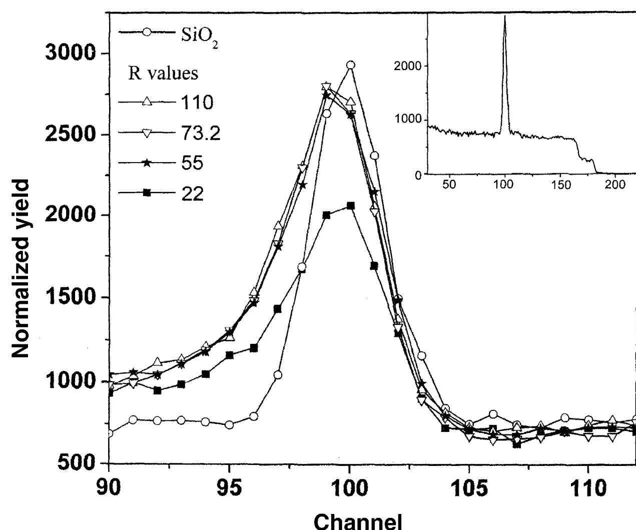

Fig. 2. The oxygen yield as obtained via the $^{16}O(\alpha,\alpha)^{16}O$ reaction for different values of R. The inset shows the whole RBS spectrum at 3.035 MeV. Typical errors are ±5%.

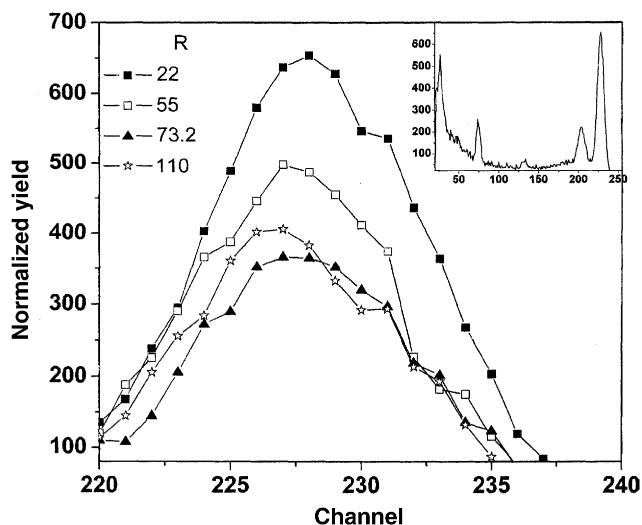

Fig. 3. The gamma yield from the $^{15}N(^{1}H;\alpha,\gamma)^{12}C$ reaction using an incident beam of 6.385 MeV $^{15}N^{2+}$ particles for the hydrogen quantification. The inset shows the whole gamma spectrum. Typical errors are ±5%.

are shown in Fig. 3. Here we observe a decrease of the gamma yield with increasing R, reaching a stable value at around $R = 72$. It was observed that for almost all R-values the H concentration remains nearly constant at around 30% level. The exception was for $R = 22$ where the H concentration reaches a 45% value (see Table 1, column 4). In one case ($R = 72$) we have investigated the H concentration over a 900 nm depth, showing to be almost constant.

The N content of the samples was determined via the $^{15}N(p,\gamma)^{16}O$ resonant reaction at $E_r = 429$ keV using the same experimental set-up as for the H case. In agreement with the Rump analysis, the N concentration was very high for $R = 22$, but became lower for the larger R values. A summary of the present results are displayed in Table 1 and in Fig. 4.

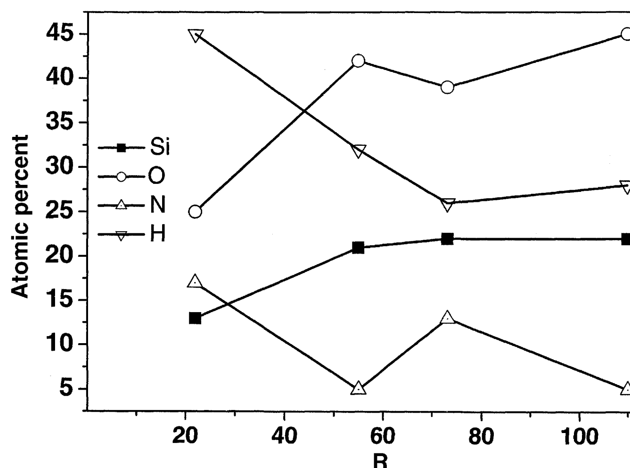

Fig. 4. Elemental composition (in percent) as a function of the R-values. Typical errors are ±5%.

As a result of the above experiments we can state the following features. First, the film density increases with R and an almost stoichiometric material was obtained for the whole analyzed R range. Second, a low and nearly constant nitrogen concentration is observed for all samples (with the exception for $R = 22$). Third, the hydrogen concentration is high for $R = 22$, decreases as R increases but still is important and almost constant for the $70 < R < 110$ interval. Since in this range the presence of bonded H-related impurities is not appreciable [4], it may be concluded that the hydrogen and nitrogen present in the samples should be mainly in the form of trapped molecules. In particular in the case of N, its stability is function of R (with exception of $R = 22$) could indicate that the bonds are saturated. This might be related to the observed dependence of the density on R.

The RBS measurements were done once for each R condition. The nuclear reactions $^{16}O(\alpha,\alpha)^{16}O$, $^{15}N(H,\alpha\gamma)^{12}C$ and $H(^{15}N,p\gamma)^{16}O$ were repeated – for each R value – at least five times. In all the cases we have obtained the same results within the experimental errors.

3.2. Surface morphology

Atomic force microscopy (AFM) images were used to study the surface roughness, grain size and shape of the samples. The AFM images (see Fig. 5) were obtained from a Multimode IIIa from Veeco microscope, operated in taping mode, using a Si cantilever ($k = 20$–50 N/m). The samples were scanned in air, over areas of 1×1 and 5×5 μm^2 with a resolution of 256×256 pixels. Before the surface analysis, the AFM images were processed using a plane fit and flatten procedure.

The grain size and shape measurements were determined by applying the Watershed technique [7], together with a shape factor algorithm [8]. The shape factor, defined as

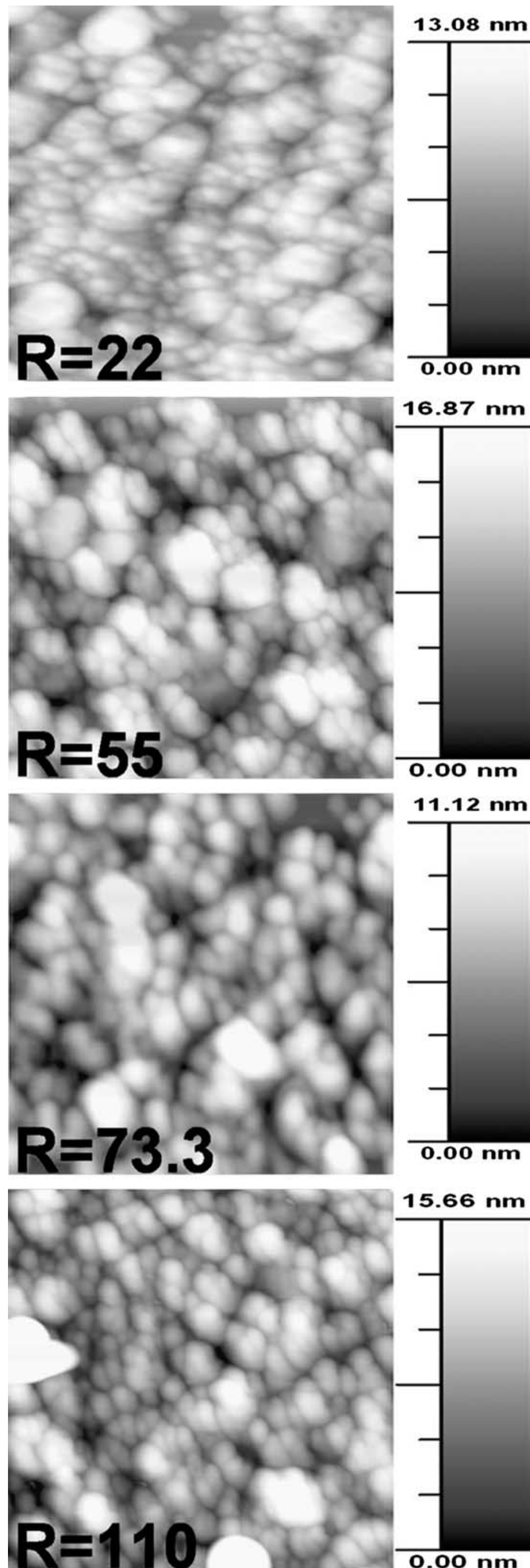

Fig. 5. AFM images corresponding to $1 \times 1\ \mu m^2$ scans.

$SF = 4\pi A/P^2$, where P is the perimeter of the grain and A its area, was used to obtain information about the shape of a grain. The surface roughness values (Rms) were also determined. For the AFM image analysis, the ImageJ v. 1.33d program [9] was used with a home developed code. The method was corroborated with the analyses made using KS400 Carl Zeiss Vision 3.0 code. The Rms and SF values were obtained from the AFM images of $5 \times 5\ \mu m^2$ scans to have a better statistics. They are shown in Table 2. It is observed that the Rms values slightly increase with R (with exception for $R = 110$). Moreover, the behavior of the SF factor indicates that the film structure follows the same dependence with R as those observed for Rms, showing only small variations as R increases.

Table 2
Surface roughness and shape factor values determined from the AFM images ($5 \times 5\ \mu m^2$ scans)

R	Rms	SF
22	2.3	0.61
55	2.4	0.60
73.3	2.5	0.66
110	4.2	0.67

One is tempted to correlate the observed surface structure to the film impurity content. However, this structure might be also related to some other phenomena associated with the deposition process, which depends on the reactant gas flow ratio. Therefore, a more complete study will be necessary to explain the observed behavior.

4. Conclusions

Ion beam analysis techniques have been successfully applied to determine the full composition of PECVD silicon oxide thin films deposited from silane and nitrous oxide as reactant gases. For precursor gas flow ratios, R, in the 22–110 interval, almost stoichiometric oxides were obtained with this deposition technique. We have shown that in this range, the type and concentration of impurities as well as the film surface morphology depend significantly on R. In addition it was observed that the film physical properties also depend on this parameter. A study of the relation between film impurity content and its physical properties is currently under progress.

Acknowledgements

This investigation was partially supported by a CNPq (Brazil) – MES (Cuba) exchange project. The authors thank the Latin American Center of Physics (CLAF) and the Brazilian agencies CNPq and CAPES for their support.

References

[1] A. Sassella, A. Borghesi, P. Corni, A. Monelli, G. Ottaviani, R. Tonini, B. Pivac, M. Bacchetta, L. Zanotti, J. Vac. Sci. Technol. A 15 (1997) 377.
[2] C.F. Lin, W.T. Tseng, M.S. Feng, J. Appl. Phys. 87 (2000) 2808.
[3] K.S. Chen, X. Zhang, S.Y. Lin, Thin Solid Films 434 (2003) 190.
[4] C. Domínguez, J.A. Rodriguez, M. Riera, A. Llobera, B. Díaz, J. Appl. Phys. 93 (9) (2003) 5125.

[5] C. Domínguez, J.A. Rodriguez, F.J. Muñoz, N. Zine, Vacuum 52 (1999) 395.
[6] L.R. Doolittle, Nucl. Instr. and Meth. B 9 (1985) 344.
[7] J. Serra, Image Analysis and Mathematical Morphology, Academic Press, London, 1988, p. 260.
[8] M. Cremona, M.H.P. Mauricio, L.C. Scavarda do Carmo, R. Prioli, V.B. Nunes, S.I. Zanette, A.O. Caride, M.P. Albuquerque, J. Microsc. 197 (2000) 260.
[9] W. Rasband, National Institute of Health, USA. Available from: <http://rsb.info.nih.gov/ij>.